

Large-Scale Generative Data-Free Distillation

Liangchen Luo*, Mark Sandler, Zi Lin*, Andrey Zhmoginov, Andrew Howard
Google Research

{luolc, sandler, lzi, azhmogin, howarda}@google.com

Abstract

Knowledge distillation is one of the most popular and effective techniques for knowledge transfer, model compression and semi-supervised learning. Most existing distillation approaches require the access to original or augmented training samples. But this can be problematic in practice due to privacy, proprietary and availability concerns. Recent work has put forward some methods to tackle this problem, but they are either highly time-consuming or unable to scale to large datasets. To this end, we propose a new method to train a generative image model by leveraging the intrinsic normalization layers' statistics of the trained teacher network. This enables us to build an ensemble of generators without training data that can efficiently produce substitute inputs for subsequent distillation. The proposed method pushes forward the data-free distillation performance on CIFAR-10 and CIFAR-100 to 95.02% and 77.02% respectively. Furthermore, we are able to scale it to ImageNet dataset, which to the best of our knowledge, has never been done using generative models in a data-free setting.

1. Introduction

Recent advances in deep learning have dramatically accelerated machine learning progress in a wide variety of artificial cognition tasks, including vision [33, 36, 45, 50], speech [17] and natural language processing [44]. One intrinsic property of deep neural networks is that they constitute a black box, with no interpretable way of describing how they perform tasks as they are trained for. While there has been significant progress in understanding how feature maps represent human interpretable features [29, 42], we still lack a complete picture of how neural networks operate. This limits our ability to extend and modify existing neural networks. Recently knowledge distillation [23, 46] has emerged as a robust way of transferring knowledge across different neural networks [6, 19, 52]. In the teacher-

student framework, the student is taught to mimic the prediction layer of the teacher. The knowledge distillation approach has been an instrumental technique for model compression [6, 19], as well as for pushing state of the art by harnessing large amounts of unlabeled data to improve the performance of student models such as Noisy Student [54] and many others, see [52] for a survey.

Despite its successes, knowledge distillation in its classical form has a critical limitation. It assumes that the real training data is still available in the distillation phase. However, in practice, the original training data is often unavailable due to privacy concerns. A typical example is medical imaging records [12, 20], whose availability is time-limited due to security and confidentiality. Similarly many large models are trained on millions [9] or even billions [39] of samples. While the pre-trained models might be made available for the community at large, making training data available poses a lot of technical and policy challenges. Even storing the training data is often infeasible for all but the largest users. Furthermore, in some training frameworks such as federated learning [31], the model is tuned by collecting gradient updates calculated on distributed devices, and the training data disappears as soon as its been used, thus requiring even more data each time the model needs to be updated.

To address this issue, a few approaches to the data-free knowledge distillation, *i.e.*, for distilling models under a data-free regime, have been previously proposed. However, they are either highly time-consuming to produce synthetic images or unable to scale to large datasets. We discuss prior research in this field in Section 2.

In this work, we adapt the idea of generative image modeling to attain efficient data generation, and investigate ways to scale it to large datasets. We propose our generative data-free distillation method, as illustrated in Figure 1, by training a generator without using the original training data and use it to produce substitute data for knowledge distillation. Our generator minimize two optimization objectives: (1) *moment matching loss*, in which the generator minimizes the difference between activation statistics and known moments estimated on training data; and (2) *incep-*

*Work done as part of the Google AI Residency.

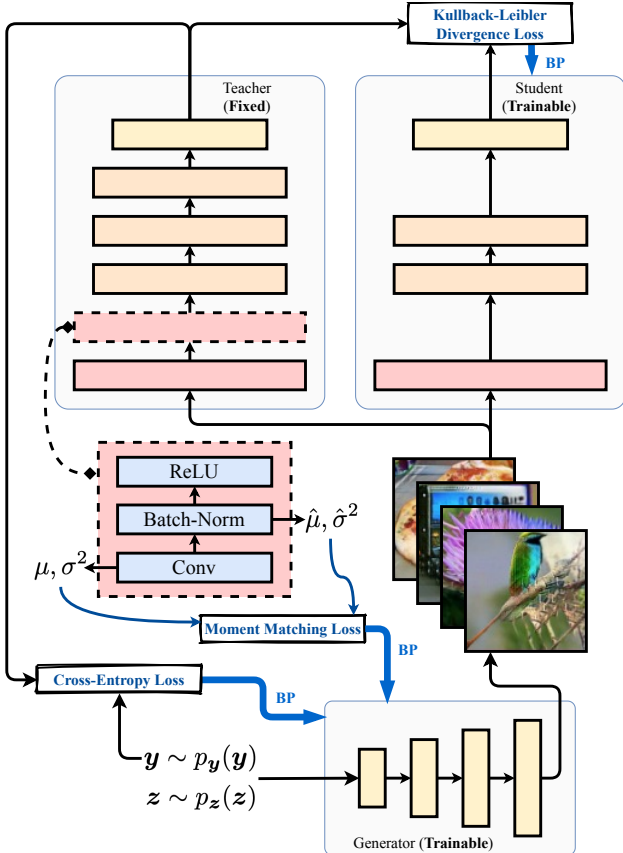


Figure 1. The proposed generative data-free distillation method. The generator is trained without the real images by (1) maximizing the probability of a target label being predicted by the pre-trained teacher; and (2) matching the statistics (μ and σ^2) of the batch-normalization (see Eq. (7)). Subsequently, the synthetic images produced by the generator enables us to apply knowledge distillation. More examples of generated images are shown in Figure 4.

tionism loss, in which the generator maximizes the activation of the logit of the teacher network corresponding to the target loss. The variants of moment-matching loss has been explored before in non-generative data-free image synthesis methods such as in [21, 55]. We also note that this information is often available as part of the training batch-normalization [26] layers which are present in nearly all modern architectures such as ResNets [22], DenseNets [25], MobileNets [24] and their variants. Under an isotropic Gaussian assumption of the internal activations, we can explicitly minimize their Kullback–Leibler divergence or the ℓ_2 -norm of their difference.

We then follow the idea of deep dream style [42] image synthesis method to employ *inceptionism loss*. The general idea is to find an input image that can maximize the probability of a certain category being predicted by the pre-trained teacher, which can be naturally formulated as a cross-entropy minimization problem. Combining this with

the aforementioned moment matching loss together, given only a pre-trained teacher model, we are now able to train a generator without using real images, which can effectively produce synthetic images for the distillation.

To demonstrate the effectiveness of the proposed method, we design an empirical study on three image classification datasets with increasing size and complexity. We first conduct an experiment of data-free distillation on CIFAR-10 and CIFAR-100. The generator trained without using real images is able to produce higher-quality and more realistic images than previous methods. These images can also effectively support the following knowledge distillation. The learned student outperforms the previous methods with a clear margin, achieving a new state-of-the-art result which is even better than its supervised-trained counterparts. We then explore using the ensemble of multiple generators on CIFAR-100 and ImageNet and demonstrate its ability of further improving the distillation result.

Our main contributions can be summarized as follows:

- We propose a new method for training an image generator from a pre-trained teacher model, which efficiently produces synthetic inputs for knowledge distillation.
- We push forward the state of the art of data-free distillation on CIFAR-10 and CIFAR-100 datasets to 95.02% and 77.02% respectively, which is even better than the supervised-trained counterparts.
- We scale the generative data-free distillation method to ImageNet by using multiple generators. This is the first success of data-free distillation on ImageNet using generative models to the best of our knowledge.

2. Related Work

Our approach can be viewed as a combination of two components, *generative modeling* and *knowledge distillation*, each of which attracted considerable attention of the deep learning community over the past years. Here we provide a brief overview of these fields in the context of our work.

Generative Image Modeling. Generative Adversarial Networks (GANs) [16], perhaps the most celebrated approach to image generation, together with numerous variants of this general method [1, 4, 28] have shown a tremendous potential for generating high-fidelity synthetic images based on a limited corpus of training samples. One appealing application of synthetic image generation is data augmentation. Recent studies have employed GAN-based augmentation to improve the model performance in data-restricted scenarios such as medical imaging [12, 20]. However, as stated in Goodfellow [15], this approach has not shown much success in practice on large-scale data. It was also observed that while the image are of extremely high

quality, using them exclusively for training leads to a significant performance degradation [55].

Another promising approach to image synthesis is based on recent work on reversible networks [3, 14, 27]. These studies explore reversible models, in which the transformation from one layer to the next are invertible, allowing to reconstruct layer activations using the outputs of the following layer. The initial motivation was to save memory by computing the activations on-the-fly during backpropagation, while later researchers have also discovered its potential for image generation [2]. We stress here, that while GAN and GAN-like methods generate very realistic and high-quality images, all aforementioned methods require access to the original data to build their generators.

Knowledge Distillation. Knowledge distillation [23] is a general technique that can be used for model compression. It transfers knowledge from a pre-trained network, the *teacher*, to another *student* network by teaching the student to mimic the teacher’s behaviour. In a typical image classification task, this is usually done by aligning the probabilities predicted by the teacher and student network. In recent literature, there have been numerous variations of knowledge distillation in terms of application domains and distillation strategies. For an overview of general distillation techniques we refer the reader to knowledge distillation surveys such as [52].

Data-Free Knowledge Distillation. The problem of knowledge distillation becomes much more challenging when the original training data is not available at the time to train the student model. This is often encountered in privacy-sensitive and data-restricted scenarios. Most approaches to this scenario center around synthetic image generation. Lopes et al. [37] was a first attempt to pre-compute and store activation statistics for each layer of the teacher network with the goal of constructing synthetic inputs that produces similar activations. Follow-up works [43, 55] have developed the approach by using less meta-data or proposing different optimization objectives. These methods typically obtain the synthetic inputs by directly optimizing some trainable random noise with regards to a pre-determined objective, where each input image requires multiple iterations to converge. Therefore, it can be costly and time-consuming to produce sufficient data for compression. There are also a few methods that synthesize input data via generative image modeling [5, 11, 41], which create substitute data much more efficiently than optimizing input noise. However, scaling them to the tasks on large datasets, e.g., ImageNet classification task, remains challenging.

3. Generative Distillation in Data-Free Setting

In this section, we first briefly recall the classical knowledge distillation method and then introduce our approach for building a generative model from a pre-trained teacher.

3.1. Notation

Generally, we denote random variables with bold serif font, e.g., \mathbf{x} , \mathbf{z} . By contrast, sampled values of such variables and deterministic tensors are denoted with regular serif font, e.g., x , which is typically used when we are discussing loss objectives with respect to a single input. Loss functions denoted by $\mathcal{L}_\blacktriangle$, where \blacktriangle is an abbreviation of a particular loss component, typically involve averaging over the probability distributions entering them. Without ambiguity, we may slightly abuse the notation of $\mathcal{L}_\blacktriangle(x)$ to denote the deterministic loss value with respect to a single input x .

3.2. Knowledge Distillation

Knowledge distillation aims to transfer knowledge from typically a larger teacher network $T(\mathbf{x}; \theta_t)$ into a smaller student $S(\mathbf{x}; \theta_s)$, where T and S are usually differentiable functions represented by neural networks with parameters θ_t and θ_s respectively and \mathbf{x} is the model input. In the setting of a classification task, T and S typically output a probability distribution over K different possible categories. The student is trained to mimic the behavior of the teacher network by matching the probability distribution produced by the teacher on the training data. Formally, knowledge distillation can be modeled as a minimization of the following objective:

$$\mathcal{L}_{\text{KD}} = \mathbb{E}_{\mathbf{x} \sim p_{\text{data}}(\mathbf{x})} [D_{\text{KL}}(T(\mathbf{x}) \parallel S(\mathbf{x}))], \quad (1)$$

where $D_{\text{KL}}(\cdot \parallel \cdot)$ refers to the Kullback–Leibler divergence that evaluates the discrepancy between the distributions produced by the teacher and student networks. Here p_{data} denotes the training data distribution.

3.3. Generative Image Modeling

Computing the loss objective in Equation (1) requires the knowledge of the data distribution p_{data} , which is not available in a data-free setting. Instead, we approximate $p_{\text{data}}(\mathbf{x})$ with a distribution of a generator trained to mimic the original data. We learn the generator distribution $p_g(\tilde{\mathbf{x}} \mid \mathbf{y})$ conditioned on the class label \mathbf{y} given the trained teacher T by introducing a latent variable \mathbf{z} with a prior $p_z(\mathbf{z})$ and representing p_g as a marginal $\mathbb{E}_{\mathbf{z} \sim p_z} \delta(\tilde{\mathbf{x}} - G(\mathbf{z} \mid \mathbf{y}))$, essentially learning a deterministic deep generator $G(\mathbf{z} \mid \mathbf{y}; \theta_g)$. The generator is then trained without the access to p_{data} , but using only the trained teacher model T . Now the key is to find appropriate objectives for training the generator. These objectives are introduced in the remainder of this section.

Inceptionism loss. Inceptionism-style [42] image synthesis, also known as DeepDream, is a way to visualize input images that provoke a particular response of a trained neural network. For instance, say we want to know what kind of image would result in “dog” class being predicted by the model. The inceptionism method would start

with a trainable image x initialized with random noise, and then gradually tweak it towards the most “dog-like” image by maximizing the probability of the dog category being produced by the model. Formally, given the expected label \hat{y} and the trained teacher T , we find x that minimizes the cross-entropy of the categorical distribution $\hat{p} = \text{OneHot}(\hat{y})$ relative to $p = T(x)$:

$$\mathcal{L}_{\text{CE}}(x, \hat{y}) = H(\hat{p}, p) = - \sum_i \hat{p}_i \log p_i. \quad (2)$$

In practice we usually do not optimize this objective alone, but also impose a prior constraint that the synthetic images mimic the statistics to the natural images, such as a particular correlation of neighboring pixels. It is done by adding a regularization term to Equation (2):

$$\mathcal{L}_{\text{Inc}}(x, \hat{y}) = \mathcal{L}_{\text{CE}}(x, \hat{y}) + \mathcal{L}_{\text{Reg}}(x), \quad (3)$$

where in this paper we follow [21, 55] to use total variation loss and ℓ_2 -norm loss as the regularizers:

$$\mathcal{L}_{\text{Reg}}(x) = \lambda_t \mathcal{L}_t(x) + \lambda_{\ell_2} \mathcal{L}_{\ell_2}(x), \quad (4)$$

where \mathcal{L}_t and \mathcal{L}_{ℓ_2} penalize the total variation and ℓ_2 -norm of the image with scaling weights λ_t and λ_{ℓ_2} , respectively.

Moment matching loss. The inceptionism loss by itself only constraints the input (images) and output (probabilities) of the trained network, while leaving the activations of internal layers unconstrained. Previous studies have observed that different layers of a deep convolutional network are likely to perform different tasks [18, 34, 38], *i.e.*, lower layers tend to detect low-level features such as edges and curves, while higher layers learn to encode more abstract features. In addition, Haroush et al. [21] showed that images learned with conventional inceptionism method may result in anomalous internal activations deviating from those observed for real data. These facts suggest there should be a regularization term to constrain the statistics of the teacher’s intermediate layers as well.

Batch normalization [26] layers, a common component of most neural networks, are helpful with providing such statistics [21, 55]. The normalization operation is designed to normalize layer activations by re-centering and re-scaling them with the moving averaged mean and variance calculated during training. In other words, it implicitly stores the estimated layer statistics of the teacher over the original data $p_{\text{data}}(x)$. Therefore, we can force the layer statistics (mean and variance specifically) produced by our synthetic images to align with those emerging from the real data [10, 48, 53].

Given the running estimates for the mean $\hat{\mu}$ and the variance $\hat{\sigma}^2$ of a teacher batch-norm layer, we measure the mean $\mu(x)$ and variance $\sigma^2(x)$ activated by the synthetic image x and minimize the discrepancy between the real-time statistics and the estimated ones. Under an isotropic

Gaussian assumption, this can be done by minimizing their Kullback–Leibler divergence:

$$D_{\text{KL}}(\mathcal{N}(\hat{\mu}, \hat{\sigma}^2) \parallel \mathcal{N}(\mu, \sigma^2)) = \log \frac{\sigma}{\hat{\sigma}} - \frac{1}{2} \left[1 - \frac{\hat{\sigma}^2 + (\mu - \hat{\mu})^2}{\sigma^2} \right], \quad (5)$$

or the ℓ_2 -norm of their differences:

$$\|\mu - \hat{\mu}\|_2 + \|\sigma^2 - \hat{\sigma}^2\|_2, \quad (6)$$

where $\mathcal{N}(\cdot, \cdot)$ stands for Gaussian distribution and $\|\cdot\|_2$ denotes the ℓ_2 -norm. In this paper, we choose the latter one and formulate the *moment matching loss* by summing up these penalties together across all the batch-norm layers:

$$\mathcal{L}_{\text{M}}(x) = \lambda_S \sum_l [\|\mu_l(x) - \hat{\mu}_l\|_2 + \|\sigma_l^2(x) - \hat{\sigma}_l^2\|_2], \quad (7)$$

where λ_S is the scaling weight and $\hat{\mu}_l, \hat{\sigma}_l^2$ are recorded mean and variance statistics for per-layer activations on the real data.

Generator training objective. Combining the inceptionism loss and moment matching loss together we get

$$\mathcal{L}_{\text{Image}}(x, y) = \mathcal{L}_{\text{Inc}}(x, y) + \mathcal{L}_{\text{M}}(x). \quad (8)$$

Recall that our final goal is to utilize these objectives to train a generative model. By substituting x with $G(z | y)$ in Equation (8), we define the final generator training objective as:

$$\mathcal{L}_{\text{G}} = \mathbb{E}_{z \sim p_z(z), y \sim p_y(y)} [\mathcal{L}_{\text{Inc}}(G(z | y), y) + \mathcal{L}_{\text{M}}(G(z | y))]. \quad (9)$$

Using multiple generators. *Mode collapse* is a common problem plaguing various generative models like GANs [16, 40, 47], where instead of producing a variety of different images, the generator produces a distribution with single image or just a few variations and the generated samples are almost independent of the latent variable. We hypothesize that in our case, if the generator occasionally produces an image corresponding to a high-confidence teacher prediction, the cross-entropy loss vanishes and the generator may learn to produce essentially only that output even if other loss components like \mathcal{L}_{M} are not fully optimized. Figure 2 illustrates a typical example of mode collapse that happened to our generator, where it is able to generate realistic images for the “automobile” class but all of the generated objects are red.

As suggested in previous literature [13, 35], training multiple generators can be a very simple but powerful way of alleviating this issue.

For our approach we choose to use a setup with k generators, and assign all classes across all generators, so that each class is assigned to exactly one generator. Each generator only tries to maximize inceptionism loss for the classes

it has assigned. For the moment matching, instead of using the moments pre-stored in batch-norm layers, in this case we use a more precise per-category moments for each generator. The way of estimating these moments is discussed in Section 4.2.



Figure 2. An example of mode collapse happened to the generator trained in data-free setting. The objects in generated images in class “automobile” are all in red color.

4. Experiments

In this section, we turn to an empirical study to evaluate the effectiveness of our method on datasets of increasing size and complexity. We first conduct a series of ablation studies on CIFAR-10 (32×32 image size; 10 categories) to verify the effect of each optimization objective for generator training, and then demonstrate the performance of using single or per-class generators on CIFAR-100 (32×32 image size; 100 categories). Finally, we extend to ImageNet (224×224 image size; 1000 categories) to show how our method scales to larger and more complex datasets.

4.1. CIFAR-10

Experimental setup. The CIFAR-10 dataset [32] consists of 50K training images and 10K testing images from 10 classes. To make a fair comparison, we follow the setting used in the previous literature [5, 11, 55] with a pre-trained ResNet-34 as the teacher network and ResNet-18 as the student. The generator architecture is also identical to the one used in [5, 11]. The generator is trained using Adam optimizer [30] with a learning rate of 0.001. We use the batch size of 256, $\lambda_S = 10$, $\lambda_{\ell_2} = 1.5 \times 10^{-5}$, and $\lambda_t = 6 \times 10^{-3}$. For CIFAR-10 we only use a single-generator mode. More details on the experimental setup can be found in the supplementary materials.

Experimental results. Test accuracies obtained using

Model	Method	Accuracy		
ResNet-34	Supervised Training	95.05% [†]		
ResNet-18	Supervised Training	93.92% [‡]		
ResNet-18	Knowledge Distillation [23]	94.34% [‡]		
ResNet-18	Gaussian Noise	11.43%		
	DAFL [5]	92.22%		
	DFAD [11]	93.3%		
	Adaptive DeepInversion [55]	93.26%		
ResNet-18	Ours	\mathcal{L}_{Inc} \mathcal{L}_M		
	◆ inceptionism	✓	77.31%	
	◆ moment matching		✓	94.61%
	◆ both	✓	✓	95.02%

Table 1. Test accuracies for different methods on CIFAR-10. [†]The test accuracy of the pre-trained teacher used in this experiment is 95.05%, while the ones used in previous literature are slightly stronger: 95.58% [5], 95.5% [11] and 95.42% [55]. [‡]As reported in [5].

different methods on CIFAR-10 are summarized in Table 1. Trained in a fully supervised setting, the teacher (ResNet-34) and the student models (ResNet-18) achieve test accuracies of 95.05% and 93.92% respectively. The student can further gain a +0.42% improvement by performing knowledge distillation on the teacher using the original training data. In the data-free setting, as was previously observed, using simple Gaussian noise as input distribution leads to a very poor performance that is only slightly better than a random guess (10%). This is not unexpected since the real data distribution looks very different from Gaussian noise and is generally expected to concentrate on a lower-dimensional manifold embedded in a high-dimensional space.

As part of our ablation study, we first trained the generator using the inceptionism loss \mathcal{L}_{Inc} alone. The resulting student model trained on this generator reached the accuracy of 77.31%, which is better than random noise, but significantly lower than the supervised accuracy of 93.92%. In another experiment, where the generator was trained with the moment matching loss \mathcal{L}_M alone, the resulting student now reached a much higher accuracy of 94.61%. Combining both objectives brings the accuracy of our final method to 95.02%, now almost indistinguishable from the accuracy of the original larger teacher model and higher than the accuracy obtained with distillation on the original training dataset.

Visualization. We finally provide several example images produced by DAFL [5], Adaptive DeepInversion (ADI) [55] and our generator in Figure 3. As we can see, although ADI can produce images with much higher quality than previous methods, it tends to synthesize images with different textures but similar background (e.g., category horse, ship and truck). In contrast, our method can generate more realistic images, which are likely to have a



Figure 3. From top to bottom, the images generated with DAFL [5], Adaptive DeepInversion (ADI) [55] and our method, respectively. The class labels are listed at the bottom.

Model	Method	Accuracy
ResNet-34	Supervised Training	77.26% [†]
ResNet-18	Supervised Training	76.53% [‡]
ResNet-18	Knowledge Distillation [23]	76.87% [‡]
ResNet-18	Gaussian Noise	1.23%
	DAFL [5]	74.47%
	DFAD [11]	67.7%
ResNet-18	Ours	
	◆ single generator	76.42%
	◆ ensembles (meta-data)	77.16%
	◆ ensembles (data-free)	77.02%

Table 2. Test accuracies of different methods on CIFAR-100. [†]The performance of the pre-trained teacher used in this experiment is 77.26%, while the ones used in previous literature are slightly stronger: 77.84% [5] and 77.5%. [‡]As reported in [5].

closer distribution to the original data.

4.2. CIFAR-100

Experiment setup. Like CIFAR-10, the CIFAR-100 dataset [32] also consists of 50K training images and 10K testing images, but the images from this dataset are categorized into 100 classes, which makes it more diverse than CIFAR-10. In most of our experiments, we use the same model architectures and training hyperparameters as in our CIFAR-10 experiments, with the only exception of λ_S now being chosen as 1. More details about the experimental setup can be found in the supplementary materials.

Single generator. Test accuracies obtained using knowledge distillation with a single generator are listed in Table 2. Our method achieves an accuracy of 76.42% on the test set, which outperforms all previous approaches by a large margin. However, this result is still slightly worse than the test accuracy of a ResNet-18 network trained in a supervised setting, or distilled from the teacher on the training data.

Multiple generators. We consider two ways of gathering per-class statistics. One direct way of accumulating it is to: (a) collect a small subset of the training images, (b) feed them to the pre-trained teacher to compute the required moments in each layer, and (c) serve them as meta-data during generator training. But although we only need a

small number of images to gather such statistics, this can no longer be thought as a purely data-free approach. In the most strict setting, where the training has to be data-free, there is another option in which we can learn several batches of trainable images using Equation (8) as the optimization objective [21, 55]. Following this approach, we can also obtain a small amount of (synthetic) images to measure per-class statistics. Specifically, we sample 100 images per class from the training data or learn the same amount of images in a data-free manner to compute the per-class statistics for each class, which is then used to train the generators. When performing distillation, we simply sample images uniformly at random from all generators.

The results of knowledge distillation with the collection of generators are shown in the last two rows in Table 2. Both methods outperform distillation with a single generator and, perhaps more remarkably, a ResNet-18 model trained in a supervised fashion, or the same model distilled on the original dataset. Finally, we see that both methods exhibit very similar performance, which suggests that we have a freedom to choose a particular approach based on the actual use case. In a scenario where we can pre-record activation statistics during the teacher training phase, it might be convenient to use the approach relying on meta-data collection. Otherwise, we may choose the alternative data-free approach without a significant loss of accuracy.

4.3. ImageNet

We finally turn to the study on ImageNet [9].

Method	Top-1 Acc.	Δ Acc.
Supervised Training	75.45%(77.26% [†])	N/A
BigGAN [4]	64.0% [‡]	-13.26%
DeepInversion [55]	68.0% [§]	-9.26%
Ours	69.75%	-5.70%

Table 3. Top-1 accuracy of different methods on ImageNet. [†]We use the ResNet-50v1 as our model while DeepInversion [55] uses ResNet-50v1.5 instead. [‡]Reported in [55]. [§]Results obtained without MixUp augmentation.

Experimental setup. The ImageNet dataset consists of

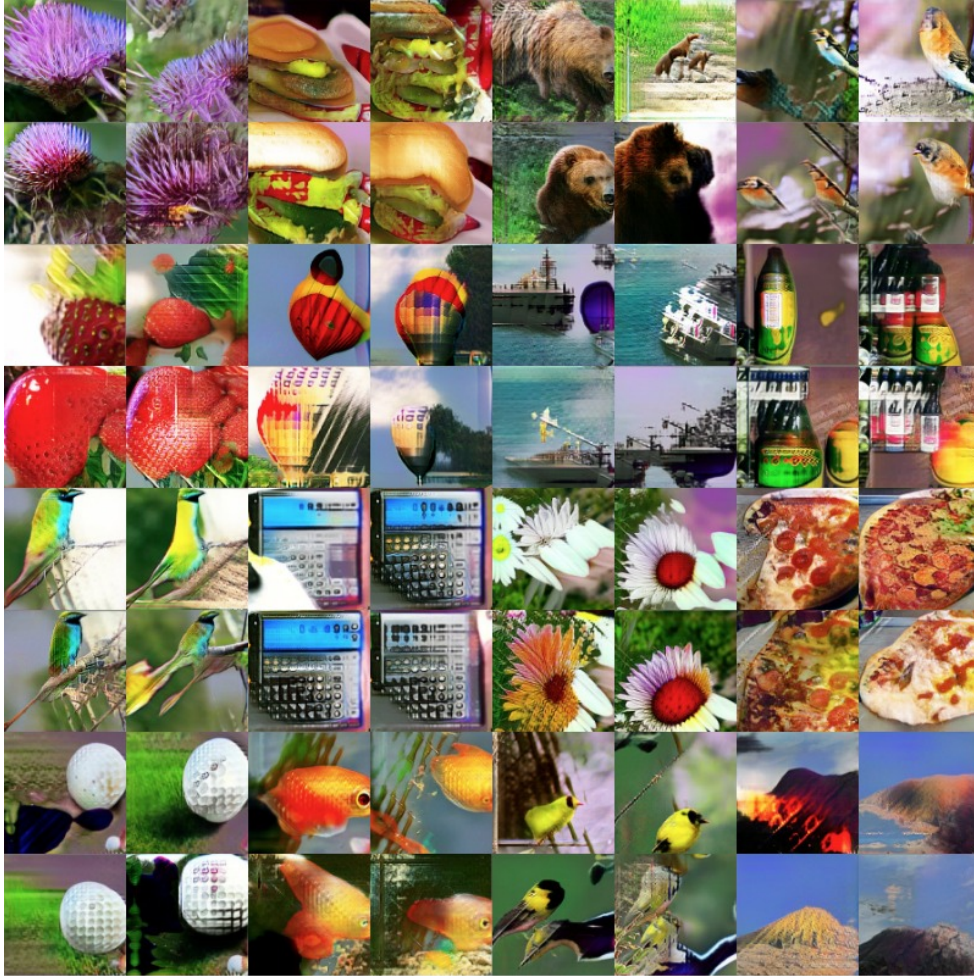


Figure 4. Examples of 224×224 images produced by the generators trained from the given teacher network. The teacher is a ResNet-50 classifier trained on ImageNet. We choose 16 categories suggested by DeepInversion [55] that images in these categories may have better visual quality. We display 4 images per category in 2×2 grids. Categories from left to right and top to down are: cartoon, cheeseburger, brown bear, brambling, strawberry, balloon, aircraft carrier, beer bottle, bee eater, hand-held computer, daisy, pizza, golf ball, goldfish, goldfinch and volcano.

over 1M images in 1000 classes. We explore two target resolutions: 32×32 matching that of CIFAR-10, and full resolution 224×224 . For 32×32 images we study the performance trade-offs between the number of generators and the accuracy. For full resolution we train an ensemble of 1000 generators for distillation, where each generator is trained to produce just a single class. The generator structure is similar to that used in CIFAR-10/100 experiment, we add additional convolutional and $2 \times$ upscaling layers to bring the image resolution to the target 224×224 . Due to memory constraints we also reduce the number of dimensions of the latent variable z from 1024 to 512. To estimate per-class statistics we sample 100 images per class. Note that this sampling can be done during the original teacher training.

All generators are trained with Adam optimizer [30] with

a learning rate of 0.001. We use the batch size of 64, $\lambda_S = 3$, $\lambda_{\ell_2} = 1.5 \times 10^{-5}$, and $\lambda_t = 6 \times 10^{-3}$. For the distillation, we use a pre-trained ResNet-50 as the teacher and distill the knowledge to several different students. We do not apply any data augmentation techniques such as Inception preprocessing [51], MixUp [56], RandAugment [8] or AutoAugment [7] for simplicity and leave further optimization as a subject of future work. More details about training setup is available in the supplementary materials.

4.4. Experimental results

Full scale ImageNet. We illustrate the test results on ImageNet in Table 3. To the best of our knowledge, this is the first distillation on Imagenet using data-free generative models, and thus no previous work in similar settings that we can directly compare with. Instead, we display the distil-

lation results using images synthesized by (1) BigGAN [4], a generative model trained with a GAN fashion on the ImageNet training data that uses real data to train generators; and (2) DeepInversion [55], which synthesizes images by directly optimizing mini-batches of trainable images one by one. Such kind of method is time-consuming to run but in theory has the potential to produce much more diverse images than using generative models. We note that DeepInversion uses ResNet-50v1.5 as the model and train it with more advanced training techniques, while we are using ResNet-50v1. As a result, the performance of our teacher is 1.8% gap to theirs in terms of top-1 accuracy, which makes the distillation results not directly comparable.

Specifically, our student trained with the ensemble of generators achieves an accuracy of 69.75%, which outperforms the ones trained with images synthesized by BigGAN and DeepInversion by 5.75% and 1.75% respectively. Considering their teacher is stronger than us by 1.81%, we actually have a even smaller gap (5.70%) to each one’s own teacher (BigGAN: 13.26%; DeepInversion: 9.26%).

Model	Method	Top-1 Accuracy
ResNet-34	Supervised Training	59.68%
ResNet-18	Supervised Training	54.99%
Ensemble of different number of generators		
ResNet-18	Ours	
	◆ #generators = 1	15.85%
	◆ #generators = 100	29.40%
	◆ #generators = 1000	51.82%

Table 4. Distillation results using ensemble of different number of generators on ImageNet 32×32 . The teacher and student are ResNet-34 and ResNet-18 respectively.

Number of generators. We further investigate the effect of the number of generators on the accuracy. Due to the computational and time constraints, we conduct this ablation study on ImageNet resized to 32×32 . We use ResNet-34 as the teacher and ResNet-18 as the student network. The single generator is trained with the moving averaged moments stored in each batch-norm layer, and the ensemble of 1000 generators is trained using per-class statistics. For the ensemble of 100 generators, we first divide the image categories into groups of 10, *i.e.*, categories 1–10 in the first group, categories 11–20 in the second group, *etc.* Then we sample 1000 images per group to estimate the per-group statistics for generator training. The setting of distillation is the same with the experiment on full-resolution ImageNet.

The results are shown in Table 4. As we can see, using a single generator we can only obtain a poor distillation accuracy of 15.85%. However by using ensembles and increasing the number of generators, we can gradually get better results and finally achieve an accuracy of 51.82%, which only has a gap of 3.17% to the supervised-trained student. These results demonstrate the importance of using ensem-

bles to scale generative data-free distillation to large dataset.

Student	Sup. Acc.	Distill. Acc.	Δ Acc.
ResNet-50	75.45%	69.75%	-5.70%
ResNet-18	68.45%	54.66%	-13.79%
MobileNetV2 [49]	70.01%	43.15%	-26.86%

Table 5. Distillation results of students with different architectures on ImageNet. The teacher is a ResNet-50 with 75.45% top-1 accuracy.

Different students. In our experiments, we also compared the distillation results on students with different architectures (see Table 5). Here the teacher is a ResNet-50 model with a top-1 accuracy of 75.45%. We use the same set of generators for all students we consider. The distillation performance on ResNet-50 is the best with an accuracy drop of 5.70% compared with the model trained in a supervised fashion. However, the performance results on ResNet-18 and MobileNetV2 [49] are much worse with larger gaps to their supervised counterparts. This indicates that perhaps there is some entanglement between student and teacher structures that make generators learned on ResNet-50 teacher to be less effective on MobileNetV2 and ResNet-18 than on ResNet-50 student. Investigation on improving its generalization ability remains subject of future work.

5. Conclusion

In this paper, we propose a new method to train a generative image model by leveraging the intrinsic normalization layers’ statistics of the trained teacher network. Our contributions are three-fold. First, we have shown that the generator trained on our proposed objectives (*i.e.*, *moment matching loss* and *inceptionism loss*) is able to produce higher-quality and more realistic images than previous methods. Second, we have successfully pushed forward the data-free distillation performance on CIFAR-10 and CIFAR-100 to 95.02% and 77.02% respectively. Finally, we were able to scale it to the ImageNet dataset, which to the best of our knowledge, has not been done using generative models before.

While we have shown that data-free distillation can successfully scale to large dataset, there are still many open questions. Specifically, our experiments with multi-category generators shows that performance drops dramatically, so generalizing our approaches to work with a single generator is a natural next step. Another direction is to utilize global moments for training images for different classes. Finally, our early experiments show that generators that we produce are teacher specific — and attempts to use them with a different teachers generally fail. It would be an important extension of our work to create universal generators that allow to learn from any teacher.

Acknowledgement

We thank Laëtitia Shao for insightful discussions, Mingxing Tan, Sergey Ioffe, Rui Huang and Shiyin Wang for feedbacks on the draft.

References

- [1] Martin Arjovsky, Soumith Chintala, and Léon Bottou. Wasserstein GAN. Jan. 2017. [2](#)
- [2] Muhammad Asim, Ali Ahmed, and Paul Hand. Invertible generative models for inverse problems: mitigating representation error and dataset bias. In *Proceedings of the 37th International Conference on Machine Learning (ICML)*, 2020. [3](#)
- [3] Jens Behrmann, Will Grathwohl, Ricky TQ Chen, David Duvenaud, and Jörn-Henrik Jacobsen. Invertible residual networks. In *Proceedings of the 36th International Conference on Machine Learning (ICML)*, pages 573–582, 2019. [3](#)
- [4] Andrew Brock, Jeff Donahue, and Karen Simonyan. Large scale GAN training for high fidelity natural image synthesis. In *Proceedings of the 7th International Conference on Learning Representations (ICLR)*, 2019. [2](#), [6](#), [8](#)
- [5] Hanting Chen, Yunhe Wang, Chang Xu, Zhaohui Yang, Chuanjian Liu, Boxin Shi, Chunjing Xu, Chao Xu, and Qi Tian. Data-free learning of student networks. In *Proceedings of the IEEE International Conference on Computer Vision (ICCV)*, pages 3514–3522, 2019. [3](#), [5](#), [6](#)
- [6] Elliot J Crowley, Gavin Gray, and Amos J Storkey. Moonshine: Distilling with cheap convolutions. In *Advances in Neural Information Processing Systems*, pages 2888–2898, 2018. [1](#)
- [7] Ekin D. Cubuk, Barret Zoph, Dandelion Mane, Vijay Vasudevan, and Quoc V. Le. Autoaugment: Learning augmentation policies from data, 2019. [7](#)
- [8] Ekin D. Cubuk, Barret Zoph, Jonathon Shlens, and Quoc V. Le. Randaugment: Practical automated data augmentation with a reduced search space, 2019. [7](#)
- [9] Jia Deng, Wei Dong, Richard Socher, Li-Jia Li, Kai Li, and Li Fei-Fei. ImageNet: A large-scale hierarchical image database. In *Proceedings of the IEEE conference on computer vision and pattern recognition (CVPR)*, pages 248–255, 2009. [1](#), [6](#)
- [10] Cícero Nogueira dos Santos, Youssef Mroueh, Inkit Padhi, and Pierre L. Dognin. Learning implicit generative models by matching perceptual features. In *2019 IEEE/CVF International Conference on Computer Vision, ICCV 2019, Seoul, Korea (South), October 27 - November 2, 2019*, pages 4460–4469. IEEE, 2019. [4](#)
- [11] Gongfan Fang, Jie Song, Chengchao Shen, Xinchao Wang, Da Chen, and Mingli Song. Data-free adversarial distillation. *CoRR*, abs/1912.11006, 2019. [3](#), [5](#), [6](#)
- [12] Maayan Frid-Adar, Idit Diamant, Eyal Klang, Michal Amitai, Jacob Goldberger, and Hayit Greenspan. GAN-based synthetic medical image augmentation for increased CNN performance in liver lesion classification. *Neurocomputing*, 321:321–331, 2018. [1](#), [2](#)
- [13] Arnab Ghosh, Viveka Kulharia, Vinay P Nambodiri, Philip HS Torr, and Puneet K Dokania. Multi-agent diverse generative adversarial networks. In *Proceedings of the IEEE Conference on Computer Vision and Pattern Recognition (CVPR)*, pages 8513–8521, 2018. [4](#)
- [14] Aidan N. Gomez, Mengye Ren, Raquel Urtasun, and Roger B. Grosse. The reversible residual network: Back-propagation without storing activations. In *Proceedings of the 31st Conference on Neural Information Processing Systems (NIPS)*, pages 2214–2224, 2017. [3](#)
- [15] Ian Goodfellow. Adversarial machine learning. Invited talk on the 33rd AAAI Conference on Artificial Intelligence, 2019. [2](#)
- [16] Ian Goodfellow, Jean Pouget-Abadie, Mehdi Mirza, Bing Xu, David Warde-Farley, Sherjil Ozair, Aaron Courville, and Yoshua Bengio. Generative adversarial nets. In *Proceedings of the 28th Conference on Neural Information Processing Systems (NIPS)*, pages 2672–2680, 2014. [2](#), [4](#)
- [17] Alex Graves, Abdel-rahman Mohamed, and Geoffrey Hinton. Speech recognition with deep recurrent neural networks. In *2013 IEEE international conference on acoustics, speech and signal processing*, pages 6645–6649. IEEE, 2013. [1](#)
- [18] Jiuxiang Gu, Zhenhua Wang, Jason Kuen, Lianyang Ma, Amir Shahroudy, Bing Shuai, Ting Liu, Xingxing Wang, Gang Wang, Jianfei Cai, et al. Recent advances in convolutional neural networks. *Pattern Recognition (PR)*, 77:354–377, 2018. [4](#)
- [19] Sangchul Hahn and Heeyoul Choi. Self-knowledge distillation in natural language processing. *arXiv preprint arXiv:1908.01851*, 2019. [1](#)
- [20] Changhee Han, Kohei Murao, Shin’ichi Satoh, and Hideki Nakayama. Learning more with less: GAN-based medical image augmentation. *CoRR*, abs/1904.00838, 2019. [1](#), [2](#)
- [21] Matan Haroush, Itay Hubara, Elad Hoffer, and Daniel Soudry. The knowledge within: Methods for data-free model compression. In *Proceedings of the IEEE/CVF Conference on Computer Vision and Pattern Recognition (CVPR)*, pages 8494–8502, 2020. [2](#), [4](#), [6](#)
- [22] Kaiming He, Xiangyu Zhang, Shaoqing Ren, and Jian Sun. Deep residual learning for image recognition. In *Proceedings of the IEEE Conference on Computer Vision and Pattern Recognition (CVPR)*, pages 770–778, 2016. [2](#)
- [23] Geoffrey Hinton, Oriol Vinyals, and Jeffrey Dean. Distilling the knowledge in a neural network. In *NIPS Workshop on Deep Learning and Representation Learning*, 2015. [1](#), [3](#), [5](#), [6](#)
- [24] Andrew G. Howard, Menglong Zhu, Bo Chen, Dmitry Kalenichenko, Weijun Wang, Tobias Weyand, Marco Andreetto, and Hartwig Adam. MobileNets: Efficient convolutional neural networks for mobile vision applications. *CoRR*, abs/1704.04861, 2017. [2](#)
- [25] Gao Huang, Zhuang Liu, Laurens Van Der Maaten, and Kilian Q Weinberger. Densely connected convolutional networks. In *Proceedings of the IEEE Conference on Computer Vision and Pattern Recognition (CVPR)*, pages 4700–4708, 2017. [2](#)
- [26] Sergey Ioffe and Christian Szegedy. Batch normalization: Accelerating deep network training by reducing internal covariate shift. In *Proceedings of the 32nd International Conference on Machine Learning (ICML)*, pages 448–456, 2015. [2](#), [4](#)

- [27] Jörn-Henrik Jacobsen, Arnold W.M. Smeulders, and Edouard Oyallon. i-RevNet: Deep invertible networks. In *Proceedings of the 6th International Conference on Learning Representations (ICLR)*, 2018. 3
- [28] Tero Karras, Timo Aila, Samuli Laine, and Jaakko Lehtinen. Progressive growing of GANs for improved quality, stability, and variation. Oct. 2017. 2
- [29] Been Kim, Martin Wattenberg, Justin Gilmer, Carrie Cai, James Wexler, Fernanda Viegas, and Rory Sayres. Interpretability beyond feature attribution: Quantitative testing with concept activation vectors (tcav), 2018. 1
- [30] Diederik Kingma and Jimmy Ba. Adam: A method for stochastic optimization. 2014. 5, 7
- [31] Jakub Konečný, H. Brendan McMahan, Felix X. Yu, Peter Richtarik, Ananda Theertha Suresh, and Dave Bacon. Federated learning: Strategies for improving communication efficiency. In *NIPS Workshop on Private Multi-Party Machine Learning*, 2016. 1
- [32] A. Krizhevsky. Learning multiple layers of features from tiny images. 2009. 5, 6
- [33] Alex Krizhevsky, Ilya Sutskever, and Geoffrey E Hinton. Imagenet classification with deep convolutional neural networks. In *Proceedings of the 26th Conference on Neural Information Processing Systems (NIPS)*, 2012. 1
- [34] Honglak Lee, Roger Grosse, Rajesh Ranganath, and Andrew Y Ng. Convolutional deep belief networks for scalable unsupervised learning of hierarchical representations. In *Proceedings of the 26th Annual International Conference on Machine Learning (ICML)*, pages 609–616, 2009. 4
- [35] Ming-Yu Liu and Oncel Tuzel. Coupled generative adversarial networks. In *Proceedings of the 30th Conference on Neural Information Processing Systems (NIPS)*, pages 469–477, 2016. 4
- [36] Jonathan Long, Evan Shelhamer, and Trevor Darrell. Fully convolutional networks for semantic segmentation. In *Proceedings of the IEEE conference on computer vision and pattern recognition (CVPR)*, pages 3431–3440, 2015. 1
- [37] Raphael Gontijo Lopes, Stefano Fenu, and Thad Starner. Data-free knowledge distillation for deep neural networks. *arXiv preprint arXiv:1710.07535*, 2017. 3
- [38] Liangchen Luo, Yuanhao Xiong, Yan Liu, and Xu Sun. Adaptive gradient methods with dynamic bound of learning rate. In *Proceedings of the 7th International Conference on Learning Representations (ICLR)*, New Orleans, Louisiana, May 2019. 4
- [39] Dhruv Mahajan, Ross Girshick, Vignesh Ramanathan, Kaiming He, Manohar Paluri, Yixuan Li, Ashwin Bharambe, and Laurens van der Maaten. Exploring the limits of weakly supervised pretraining. In *Proceedings of the European Conference on Computer Vision (ECCV)*, pages 181–196, 2018. 1
- [40] Qi Mao, Hsin-Ying Lee, Hung-Yu Tseng, Siwei Ma, and Ming-Hsuan Yang. Mode seeking generative adversarial networks for diverse image synthesis. In *Proceedings of the IEEE Conference on Computer Vision and Pattern Recognition (CVPR)*, 2019. 4
- [41] Paul Micaelli and Amos J Storkey. Zero-shot knowledge transfer via adversarial belief matching. In *Advances in Neural Information Processing Systems*, pages 9551–9561, 2019. 3
- [42] Alexander Mordvintsev, Christopher Olah, and Mike Tyka. Inceptionism: Going deeper into neural networks, 2015. 1, 2, 3
- [43] Gaurav Kumar Nayak, Konda Reddy Mopuri, Vaisakh Shaj, Venkatesh Babu Radhakrishnan, and Anirban Chakraborty. Zero-shot knowledge distillation in deep networks. In *International Conference on Machine Learning*, pages 4743–4751, 2019. 3
- [44] D. W. Otter, J. R. Medina, and J. K. Kalita. A survey of the usages of deep learning for natural language processing. *IEEE Transactions on Neural Networks and Learning Systems*, pages 1–21, 2020. 1
- [45] Shaoqing Ren, Kaiming He, Ross Girshick, and Jian Sun. Faster R-CNN: Towards real-time object detection with region proposal networks. In *Proceedings of the 29th Conference on Neural Information Processing Systems (NIPS)*, pages 91–99, 2015. 1
- [46] Adriana Romero, Nicolas Ballas, Samira Ebrahimi Kahou, Antoine Chassang, Carlo Gatta, and Yoshua Bengio. Fitnets: Hints for thin deep nets. *arXiv preprint arXiv:1412.6550*, 2014. 1
- [47] Tim Salimans, Ian Goodfellow, Wojciech Zaremba, Vicki Cheung, Alec Radford, and Xi Chen. Improved techniques for training GANs. In *Proceedings of the 30th Conference on Neural Information Processing Systems (NIPS)*, pages 2234–2242, 2016. 4
- [48] Tim Salimans, Ian J. Goodfellow, Wojciech Zaremba, Vicki Cheung, Alec Radford, and Xi Chen. Improved techniques for training gans. In Daniel D. Lee, Masashi Sugiyama, Ulrike von Luxburg, Isabelle Guyon, and Roman Garnett, editors, *Advances in Neural Information Processing Systems 29: Annual Conference on Neural Information Processing Systems 2016, December 5-10, 2016, Barcelona, Spain*, pages 2226–2234, 2016. 4
- [49] Mark Sandler, Andrew Howard, Menglong Zhu, Andrey Zhmoginov, and Liang-Chieh Chen. MobileNetV2: Inverted residuals and linear bottlenecks. In *Proceedings of the IEEE Conference on Computer Vision and Pattern Recognition (CVPR)*, pages 4510–4520, 2018. 8
- [50] Karen Simonyan and Andrew Zisserman. Very deep convolutional networks for large-scale image recognition. In *Proceedings of the 3rd International Conference on Learning Representations (ICLR)*, 2015. 1
- [51] Christian Szegedy, Sergey Ioffe, and Vincent Vanhoucke. Inception-v4, Inception-ResNet and the impact of residual connections on learning. *CoRR*, abs/1602.07261, 2016. 7
- [52] Lin Wang and Kuk-Jin Yoon. Knowledge distillation and Student-Teacher learning for visual intelligence: A review and new outlooks. Apr. 2020. 1, 3
- [53] David Warde-Farley and Yoshua Bengio. Improving generative adversarial networks with denoising feature matching. In *5th International Conference on Learning Representations, ICLR 2017, Toulon, France, April 24-26, 2017, Conference Track Proceedings*. OpenReview.net, 2017. 4
- [54] Qizhe Xie, Minh-Thang Luong, Eduard Hovy, and Quoc V. Le. Self-training with noisy student improves imagenet classification, 2020. 1
- [55] Hongxu Yin, Pavlo Molchanov, Jose M Alvarez, Zhizhong

Li, Arun Mallya, Derek Hoiem, Niraj K Jha, and Jan Kautz. Dreaming to distill: Data-free knowledge transfer via Deep-Inversion. In *Proceedings of the IEEE/CVF Conference on Computer Vision and Pattern Recognition (CVPR)*, pages 8715–8724, 2020. [2](#), [3](#), [4](#), [5](#), [6](#), [7](#), [8](#)

[56] Hongyi Zhang, Moustapha Cisse, Yann N. Dauphin, and David Lopez-Paz. mixup: Beyond empirical risk minimization, 2018. [7](#)

Appendix

A. Experiment Settings

We provide more experimental details in this section. Generally, each generator is trained on an NVIDIA V100 GPU for 10K steps using the Adam optimizer with $\beta_1 = 0.9$, $\beta_2 = 0.999$, $\epsilon = 1 \times 10^{-8}$ and a constant learning rate of 0.001. We run all the knowledge distillation experiments on a Cloud TPUv3 32-core Pod slice. We use the Momentum optimizer and set the momentum parameter to 0.9. We employ a linear warm-up scheme where the learning rate increases from 0 to the base learning rate for the first 5K training steps, and then it is decayed by 0.977 every 1K steps. The temperature of distillation is set to 3.

A.1. CIFAR-10

We run knowledge distillation for 60K steps with a batch size of 32768 and base learning rate of 0.06. The generator architecture is illustrated in Table 6, where $K = 10$.

A.2. CIFAR-100

We run knowledge distillation for 60K steps with a batch size of 32768 and base learning rate of 0.1. The generator architecture is illustrated in Table 6. For the single-generator experiment, $K = 100$. On the other hand, in multiple-generators experiment, each generator is responsi-

ble for producing images in a certain category, and therefore $K = 1$.

A.3. ImageNet

We run knowledge distillation for 300K steps with a batch size of 2048 and base learning rate of 0.1. For the target resolution of 32×32 , we use the same generator architecture as the one used in CIFAR-10/100 experiments. For the full resolution (224×224), each generator is responsible for producing images in one category, whose architecture is illustrated in Table 7.

$z \in \mathbb{R}^{1024} \sim \mathcal{N}(0, I)$
$\text{OneHot}(y) \in \mathbb{R}^K$
Linear($1024 + K$) $\rightarrow 8 \times 8 \times 128$
Reshape, BN, LeakyReLU
Upsample $\times 2$
3×3 Conv 128 $\rightarrow 128$, BN, LeakyReLU
Upsample $\times 2$
3×3 Conv 128 $\rightarrow 64$, BN, LeakyReLU
3×3 Conv 64 $\rightarrow 3$, Tanh

Table 6. Generator architecture for CIFAR-10 and CIFAR-100. K denotes the number of classes, where $K = 10$ for CIFAR-10 and $K = 100$ for CIFAR-100 in single-generator mode; and $K = 1$ for the multiple generators experiment.

$z \in \mathbb{R}^{512} \sim \mathcal{N}(0, I)$
Linear(512) $\rightarrow 7 \times 7 \times 64$
Reshape, BN, LeakyReLU
Upsample $\times 2$
3×3 Conv 64 $\rightarrow 64$, BN, LeakyReLU
3×3 Conv 64 $\rightarrow 3$, Tanh

Table 7. Generator architecture for ImageNet.